

CO₂ EMISSION TRENDS AND RISK ZONE MAPPING OF FOREST FIRES IN SUBTROPICAL AND MOIST TEMPERATE FORESTS OF PAKISTAN

MANNAN, A.^{1,2} – FENG, Z.^{1,3*} – AHMAD, A.^{4,5} – BECKLINE, M.⁴ – SAEED, S.⁴ – LIU, J.^{1,3} – SHAH, S.³ – AMIR, M.⁶ – AMMARA, U.⁷ – ULLAH, T.⁸

¹*Beijing Key Laboratory of Precision Forestry, Beijing Forestry University, Beijing 100083, China*

²*Forest, Wildlife and Fisheries Department, Government of Punjab, Lahore 54500, Pakistan*

³*State Forestry Administration, Key Laboratory of Forest Resources and Environmental Management, Beijing Forestry University, Beijing 100083, China*

⁴*Laboratory of Integrated Forest Management, School of Forestry, Beijing Forestry University Beijing 100083, China*

⁵*Shaheed Benazir Bhutto University, Sheringal Dir Upper, KPK Pakistan*

⁶*Beijing Key Laboratory of Forest Resources and Ecosystem Process, College of Forestry, Beijing Forestry University, 100083 Beijing, China*

⁷*Department of Environmental sciences, International Islamic University, Islamabad, Pakistan*

⁸*School of Nature Conservation, Beijing Forestry University, Beijing, China*

**Corresponding author*

e-mail: fengzhongke@126.com; phone/fax: +86-138-1156-5523; address: No. 35, Tsinghua East Road, Haidian District, Beijing, P. R. China

(Received 25th Nov 2018; accepted 16th Jan 2019)

Abstract. Due to high temperatures and dry summer in most subtropical regions, forest fires are of a regular occurrence. Fires emit CO₂ and other greenhouse gases which retroact on the ecological systems. This study provides CO₂ emission estimates from forest fires and risk zones in subtropical and temperate forests of Pakistan. CO₂ emission was calculated using average dry matter g/m², burned area, combustion factor (CF) and burning efficiency (E_f) following the guidelines of Inter-governmental Panel on climate change (IPCC). Fire risk zones were created by using GIS tools considering anthropogenic and natural geological factors. Results showed that average dry organic matter is 13837 ± 5774.64 gm⁻², while average annual CO₂ emission is 7280 ± 5369 Gg with 56.6% average annual increase of CO₂ emission. Meanwhile, highest emission of about 22799 Gg was recorded in 2009 corresponding to about 145.6 ha of burnt forests. Additionally, over 56% of the area or 9.33% (extreme risk zone) and 45.20% (high risk zone) is threatened by fire. Forest fire trends are mainly due to an increase anthropogenic activities and changes in weather conditions. Understanding forest fire threats and trends, will aid the government authorities in making appropriate conservation programs to curtail these forest fire threats and carbon dioxide emission trends.

Keywords: *burnt biomass, burning efficiency, Murree forest division, remote sensing, risk assessment*

Introduction

Globally, human activities and forest fires continue to reduce forest cover. This forest cover change distorts the forest and surrounding ecosystem functions, biodiversity conservation and hence forest regeneration (Tanvir et al., 2006; Beckline

and Yujun, 2014). Forest fires occur at regular intervals and reduce plant growth and regeneration hence exacerbating soil erosion (Jaiswal et al., 2002; Mukete, 2018a).

Forest fires are also deleterious to trees where trees become more susceptible to fungal and insect attacks thus affecting wood quality and volume (Abd El-Kawya et al., 2011). Globally, tree cover loss was observed to have attained a record 2.97 million km² in 2016 (Weisse and Goldman, 2017), the loss is 51% higher than the previous year with forest fires being the primary cause of this spike. In the Brazilian Amazonian region tree cover loss was estimated at over 370,000 km² nearly three times more than in 2015, this increase mainly occurred in the states of Pará and Maranhão, which were heavily affected by fire in late 2015 and early 2016 (Chanthathath, 2017)

Forest fires are the greatest potential risk to stored terrestrial carbon and each year an estimated 2-3 PgC are released into the atmosphere corresponding to about 3-4 million km² of burnt forests (Giglio, 2006; Hansen et al., 2013; Weisse and Goldman, 2017). Forest fires cause changes in the earth's biological and physical characteristics which over the years, affect carbon exchange (Harden et al., 2000; Vilen and Fernandes, 2011). According to Wekesa et al. (2016), about 82-97% of released carbon dioxide (CO₂) constitutes total carbon stock. Therefore, emission of greenhouse gases such as CO₂ and methane (CH₄) from forest fires directly affects climate (Simpson et al., 2006; Hansen et al., 2013)

Forest fire risk zones are areas from where a fire is likely to have started and spreads to other areas (Leblon, 2005). The availability of forest fire risk zone mapping aids in the precise evaluation of the fire (Jaiswal et al., 2002). This risk-mapping involves the multi-criteria evaluation method that includes factors such as slope, elevation, aspect, land-use, climatic conditions, proximity to roads and settlements (Bacani, 2016; Mukete et al., 2018b). One of the most common practices of risk zoning is the assigning of the subjective layer to all classes according to the sensitivity of fire and ignition capabilities (Dong et al., 2005). For instance, Ito and Penner (2004) used GIS-grid based system and multi-criteria to map peat swamp forests in Pekan District, south of Pahang, Malaysia to develop weighted fire index model for fire hazards. However different studies use different methods such as meteorological data and occurrence of forest fires for the establishment of forest fire models and risk zone assessment (Alonso-Betanzos et al., 2003; Zhang et al., 2011). The other studies have developed forest fire models by maintaining environmental and physiographic factors that affect the wildfire (Mitchener and Parker, 2005; Thompson et al., 2017). Similarly, the combination of satellite remote sensing and modeling have opened up new opportunities for the quantitative assessment of pre and post- forest fires.

In Pakistan, sub-tropical and temperate forests are located in the northern part of the country along the Himalayan foothills (Mannan et al., 2018a; Amir et al., 2018). This dry sub-tropical climate makes sub-tropical and temperate forests vulnerable to forest fires. This is particularly from altitudinal variations which influence the spreading of forest fires at different elevations (Ali, 2013; Saeed et al., 2019). In Pakistan, each year a considerable area of subtropical and moist temperate forests come under fire mainly due to natural causes, human and accidents. According to FAO (2015) and Hansen et al. (2013) more than 80% fires in these forests are due to anthropogenic activities.

Although biotic and abiotic factors facilitate the assessment of heterogeneous distribution and occurrence of fire density, Pakistan lacks active fire management plans both at regional and national levels. These limits and diffuses the control and monitoring of the increasing trends in national carbon emissions (Krawchuk et al.,

2009; Saeed et al., 2016, 2018; Mannan et al., 2018b; Adnan et al., 2018) which has therefore necessitated an urgent need for national fire management plans. This study strives to fill this knowledge gap by estimating carbon emissions in the subtropical and temperate forests of Pakistan. It focuses on carbon emission trends within the last two decades as well as the anthropogenic, topographic and climatic factors. Understanding forest fire threats and trends, will aid the competent government authorities in developing appropriate conservation policies such as to curtail these forest fire threats and carbon dioxide emission trends.

Materials and methods

Description of study area

The subtropical and moist temperate forests are primarily located at the foot of the Himalayan mountain ranges (550-2600 altitude) between 33° 46' 50.60" N to 33° 56' 01.48" N latitude and 73° 09' 36.76" E to 73° 33' 29.66" E longitude (Ashraf et al., 2014), as shown in *Figure 1*. The area spreads across over 46898 ha and it is administratively controlled by Murree Forest Division (MFD) and includes three forest types. These are subtropical broad-leaved evergreen forests, subtropical Chir pine forests and moist temperate forests. Common plant species include *Pinus roxburghii* (Chir-pine), *Pinus wallichiana* (Blue pine), *Abies spp*, *Cedrus deodara* (Diar), *Quercus incana* (Oak), *Aesculus indica* (Chentnut), *Dodonea spp* (snatha), *Olia spp* (Indian olive) (Shahzad et al., 2015)

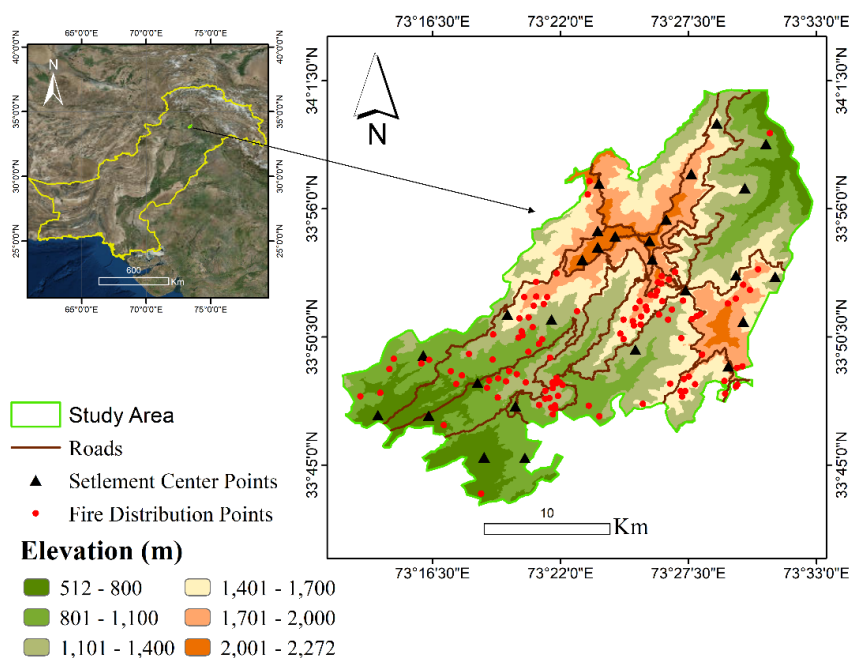


Figure 1. Map of the study area, showing fire distribution, settlements centre points and roads

The mean annual precipitation is 1800 mm, the mean annual max and min temperature are 24.3 °C and 11.4 °C, while the mean annual relative humidity is 53.06%, mean annual wind velocity is 3.22 km/h and mean annual solar energy is 18.4 J

(PMD, 2015). Geologically the study area is composed of Cretaceous and Tertiary sedimentary strata having deep relief due to tectonic uplift during the tertiary period (Ashraf et al., 2014).

Data acquisition

The image of the study area was obtained from satellite (Sentinel-2), the cloud free image of 22nd October, 2017 was selected that is freely available on European space agency (ESA) website <https://sentinel.esa.int/web/sentinel/home>, topographic maps at scale of 1:25000 of the study area was obtained from survey of Pakistan (<http://www.surveyofpakistan.gov.pk/>). Digital elevation model (DEM) with the 30 m resolution was obtained from United States Geological Survey (USGS) <https://earthexplorer.usgs.gov/>. Forest type map, forest fire data (1998-2017) and Fire watch tower information were obtained from the office of the Murree forest division (MFD). Roadmap of Murree was obtained from National Highway Authority Islamabad (NHA) and Settlements map from the office of Pakistan Statistical Bureau (PSB) as shown in *Table 1*. The field data were collected by taking sample plots randomly distributed in the study area for biomass and CO₂ emission calculations.

Table 1. Dataset and sources

Data	Source	Abbreviation	Unit/resolution/Scale
Sentinel-2	European Space Agency (ESA)	Sent-2	10 m
Digital elevation model	Earth explorer (USGS)	DEM	30 m
Topographic map	MFD (Punjab forest department)	MFD	1:25000
Elevation	Derived from DEM	Elev	Meters (m)
Aspect	Derived from DEM	Asp	Classes 1-4
Slope	Derived from DEM	Slope	Classes 1-4
Distance from roads	Rod map from (NHA)	DisRd	Meters (m)
Distance from settlements	Settlements map from SBP	DisSet	Meters (m)
Watch towers	MFD	MFD	
Mean Annual Precipitation	PMD &NOAA	mm	Millimeters (mm)
Mean Annual Temperature	PMD &NOAA	Temp	Degree centigrade (°C)
Land-uses	From Satellite Image	Land-use	30 m

Biomass and CO₂ emission estimation

A total of 150 plots of size 20 m × 30 m were randomly sampled as shown in *Figure 2* and the stem volume (m³/ha) measured for all the trees found within. In each sample plot, the diameter of all trees greater than 4 cm was measured at breast height (DBH). Using the Abney level, the height of 20 trees per species was recorded which were used to construct DBH/height function of a specific plot.

We first arranged the trees present in the sample plot into different classes based on their diameter (Dia classes), density of each diameter class i.e. no of trees per hectare were calculated and the basal area (B.A) of each diameter class was by using *Equation 1*.

$$B.A = \text{Density} \times DBH \times \pi r^2 \left(\frac{m^2}{ha} \right) \quad (\text{Eq.1})$$

Stem volume was measured using *Equation 2* as described by Newbery (2009).

$$\text{Stem Volume} \left(\frac{m^3}{ha} \right) = B.A \left(\frac{m^2}{ha} \right) \times h(m) \times f.f \quad (\text{Eq.2})$$

where B.A is the basal area, h is height and form factor f.f is the volume of cylinder to actual tree form (Tenzin et al., 2017). In the Indian sub-continent, f.f is usually 0.37 for conifers and 0.6 for broad leaves is commonly used (Haripriya, 2002). Biomass t/ha was calculated by multiplying stem volume with the wood density (W.D) t/m³ of particular species using IPCC proposed guidelines (IPCC, 2006b). The wood density values were also confirmed by previous research and reports (Sheikh, 1993; *Eq. 3*).

$$\text{Stem Biomass} \left(\frac{t}{ha} \right) = \text{Stem Volume} \left(\frac{m^3}{ha} \right) \times W.D \left(\frac{t}{m^3} \right) \quad (\text{Eq.3})$$

Total Biomass t/ha (above ground biomass, understory vegetation biomass, litters and dead wood) was measured by using Biomass expansion factor (BEF) for subtropical and temperate forests of Pakistan as described by Haripriya (2002) and IPCC (2006a) (*Eq. 4*).

$$\text{Total Biomass} \left(\frac{t}{ha} \right) = \text{Stem Biomass} \left(\frac{t}{ha} \right) \times BEF \quad (\text{Eq.4})$$

Biomass carbon values of understory vegetation (USV) were measured by establishing sub-plot of 4 m × 4 m in each sample plot; the USV vegetation includes herbs, weeds, and grasses etc. The vegetation in each sub-plot was harvested by using sickle. The average fresh weight of the harvested material in kg/m² was recorded and all harvested vegetation was put into brown paper labeled bags. Then the paper bags were dried in gravity convection oven, model no (SG03) at 72 °C for 48 h and their dried weights in kg/m² were measured for Biomass Carbon Calculation. Similarly, we collected litter; dead wood and cones present in the sub-plot and measure the average weight kg/m². Tree biomass, USV biomass, litters and deadwood were added and the total biomass t/ha was calculated (Brown et al., 1982; Saugier et al., 2001; Malhi et al., 2004; Vilen and Fernandes, 2011), as shown in *Equation 5*.

$$\text{Average dry organic matter } B \left(\frac{g \text{ dm}^2}{m^2} \right) = \text{Average Biomass} \left(\frac{t}{ha} \right) \times 100 \quad (\text{Eq.5})$$

B is the average organic matter in particular ecosystem per unit area (g dm/m²), after the dry organic matter was calculated, we used (Seiler and Crutzen, 1980; Vilen and Fernandes, 2011) formula for the calculation of total burned biomass (BBM) as shown in *Equation 6*.

$$BBM = A \times B \times CF \quad (\text{Eq.6})$$

BBM is the burned dry biomass (g dry matter per unit time) in particular ecosystem burned. Where A is the annually burnt area m²/year, B is Average organic matter per unit area g/m² and CF is the Combustion factor or biomass burning efficiency. Combustion factor is the exposed biomass that is actually consumed during combustion (Ito and Penner, 2004). Only a portion of the biomass is burnt but most biomass remains in the form of standing trees, charcoal or dead organic matter. This handicap was resolved by using 0.74 combustion factor for subtropical/tropical grasslands and 0.45 for temperate forests according to guidelines of IPCC (2006a; Eq. 7).

$$E_c = BBM \times E_{fc} \quad (\text{Eq.7})$$

The total burnt biomass BBM was then converted into emitted CO₂ by using the equation, where the CO₂ emission factor (E_{fc}) that described the weight of CO₂ emitted per weight of dry burnt biomass. The amount of released compound by the amount of dry fuel consumed g/kg of dry fuel consumed is the emission factor (Andreae and Merlet, 2001; Saranya et al., 2016). According to IPCC (2006a) the emission factor E_{fc} 1531 g/kg for sub-tropical and temperate region is used to calculate the average annual carbon emission for the last two decades (1998-2017).

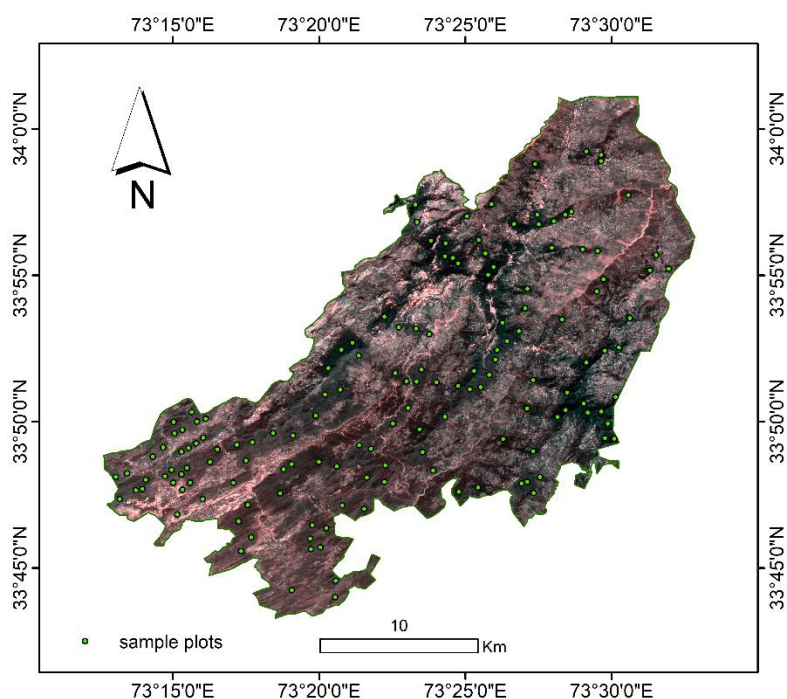


Figure 2. Sample plots distribution

Forest fire risk zoning and fire risk index

Forest fire risk zone map was generated by using vegetation type (broad-leaved forest, chirpine forest, and moist temperate forest), land-use (dense forest (DF), open forest (OF), bare land (BL), settlements (SM), agricultural land (AL), topography (slope, aspect, elevation), human factors (distance from roads, distance from settlements) and watch tower visibility in MFD. The topographic sheet of the study area

and forest distribution map at the scale of 1:25000 of the study area was obtained from the office of the MFD. The topographic map and forest distribution map were scanned and exported into the processing software ArcGIS 10.2 and ENVI 5.1. The Shapefile was clipped by using the topographic sheet as a reference. Sentinel-2 image having 10 m resolution was downloaded for European space agency (ESA). First, the image pre-processing was performed in ENVI 5.1 and the geometric distortion of the image was removed from the topographic sheet as well as from the GPS by selecting 20 Ground Control Points (GCPs) around the study area. Image pre-processing is necessary before the classification or distribution for establishing a relationship between acquired data and biophysical processes (Abd El-Kawy et al., 2011; Iwan et al., 2004; Mannan et al., 2018). The geometrically corrected image was then used to clip the region of interest (ROI). After that, the image was classified into five different classes such as dense forest (DF), open forest (OF), agricultural land (AL), settlements (SM), and barren land (BL), Road (RD) with corresponding classes by assigning per-pixel signatures. On the bases of different digital number (DN) value of landscapes different colours assigned to differentiate them. After that Radiometric, the atmospheric and topographic correction was performed by using ArcGIS 10.2 and ENVI 5.1.

Training samples for each predetermined class were selected by delimiting polygons and spectral signatures for each land cover type derived from satellite imagery were recorded using pixels inside polygons. Supervised classification was performed by using a maximum likelihood algorithm. Accuracy of the land-use change was assessed by using confusion matrix in ENVI 5.1. We took 50 ground truth points in each land-use, for accuracy assessment. The kappa statistics was calculated by using *Equation 8*.

$$K (kappa) = \frac{Observed - Expected}{1 - Expected} \quad (Eq.8)$$

To improve the quality of classification and to classify the un-classed pixels, post classification smoothing was performed. Post classification smoothing is used to improve the classification quality, un-classified pixel (Harris and Ventura, 1995). The Land cover classification as shown in *Figure 6a*, gives meaningful information about the class value and also links the spectral characteristics of the image, that can be displayed as a map for researchers and scientists to evaluate the land-use classes (Weber and Dunno, 2001).

Spatial distribution and statistics of forest type were calculated from forest distribution map (*Fig. 7a*). The forest distribution map was first scanned imported to processing software ArcGIS 10.2. Geometric correction of the map was performed from the topographic sheet by selecting 50 Ground Control Points (GCP's) around the study area, DEM (30 m) was used to calculate the slope, elevation and aspect, as shown in *Figure 8a, b, c*. Reclassification tool was used for making their risk zone classes. Roadmap and settlements map of MFD was obtained from NHA and PBS, which was used to construct fire risk distance corridors. Euclidian distance tool in ArcGIS 10.2 was used for making 100 m, 200 m, 300 m and 400 m corridors of roads and settlement center points of the study area (see *Fig. 7b*).

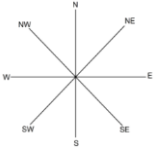
For Fire rating index (FRI) determining first of all the risk ratings were assigned to the variable factors responsible for forest fire according to their fire causing potential, which was determined by referring previous research and historical record, as shown in *Table 2*. The higher rating shows that variable has a high influence on fire risk. Secondly, each variable is classified into classes i.e. (extreme, high, moderate, low and

no risk) and finally all the layers were integrated through GIS and by using Equation 9 FRI is calculated.

$$FRI = 10(lu_i + ft_j) + 5sl_k + 3asp_l + 2ele_m + 2set_n + 2rd_o \quad (\text{Eq.9})$$

In FRI, *lu* is the land-use having (6 classes), *sl* is slope factor (4 classes), *asp* is aspect (9 classes), *ele* is elevation (4 classes), *set* is distance from settlements (4 classes) and *rd* is the distance from roads (4 classes). The superscripts (*i,j,k,l,m,n,o*) are the sub-classes. Finally, weighted overlay tool was used for overlay analysis and all the layers were combined to form final fire risk zone map of the study area shown in Figures 3 and 10.

Table 2. Fire hazard factors

Factors	Classes	Assigned value	Risk factor
Land-use (10)	Dense forest	5	Extreme
	Open forest	4	High
	Barren land	1	No risk
	Agricultural land	3	Moderate
	Roads	1	No risk
	Water	1	No risk
	Settlements	1	No risk
Forest type (10)	Sub-tropical broad leave evergreen forest	4	High
	Subtropical Chir pine (<i>Pinus roxburghii</i>) forest	5	Extreme
	Moist temperate forest	3	Moderate
Elevation (2)	500-1000 m	5	Extreme
	1000-1500 m	4	High
	1500-2000 m	3	Moderate
	2000-2500 m	2	Low
Slope (5)	0-10°	2	Low
	11-20°	3	Moderate
	21-40°	4	High
	<41°	5	Extreme
Aspect (3) 	N (0-22.5)	2	Low
	NE (22.5-67.5)	3	Moderate
	E (67.5-112.5)	3	Moderate
	SE (112.5-157.5)	4	High
	S (157.5-202.5)	5	Extreme
	SW (202.5-247.5)	5	Extreme
	W (247.5-292.5)	3	Moderate
	NW (292.5-337.5)	3	Moderate
	N (337.5-360)	2	Low
	Distance from settlements (2)	0-100 m	5
100-200 m		4	High
300-400 m		3	Moderate
400-500 m or >		2	Low
Distance from roads (2)	0-100 m	5	Extreme
	100-200 m	4	High
	200-300 m	3	Moderate
	300-400 m or >	2	Low

Visibility analysis

Fire watch towers are very important for early detection of forest fires. There are two fire watch towers in the study area which include the 17 m high and 12 km maximum range of visualization Ban fire tower and the 20 m high and 15 km of maximum visualization range Charihan fire tower. The visibility analysis of the study area was carried out with the view-shed tool in ArcGIS 10.2 by using DEM and fire towers geographical location (Fig. 9 and Table 3)

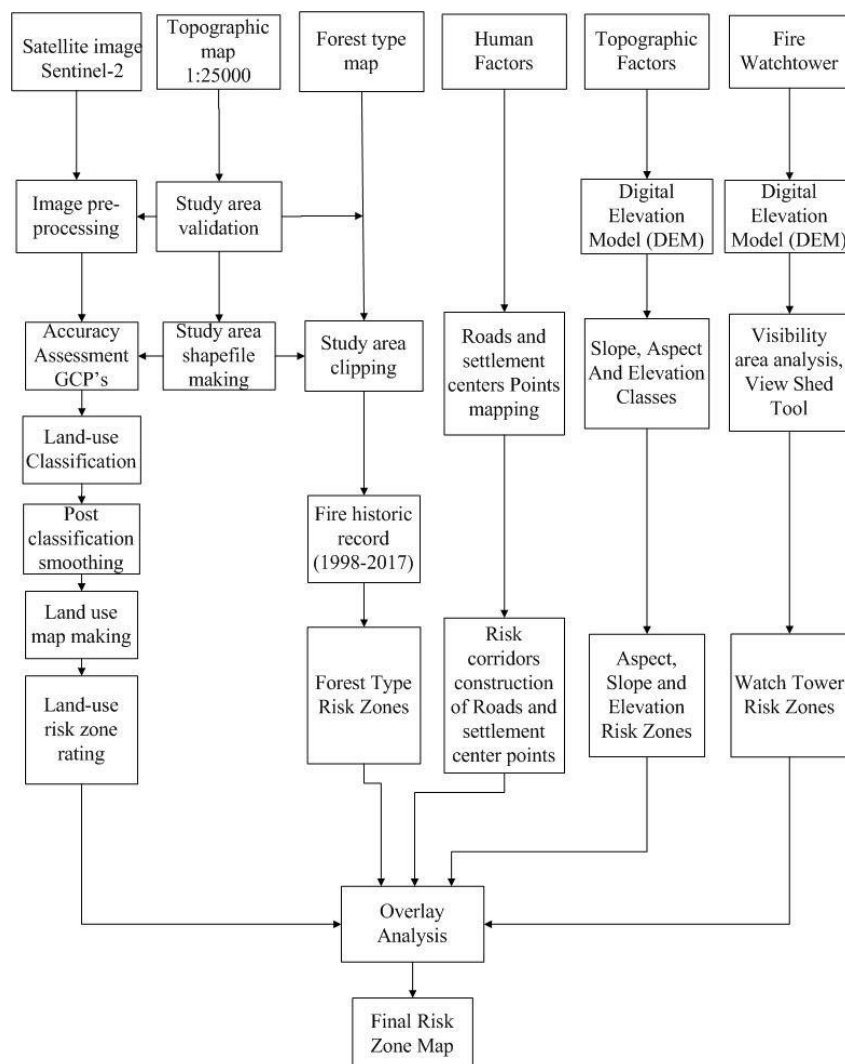


Figure 3. Flow Chart

Table 3. Visibility analysis of the study area

Towers	Visible area		Invisible area	
	Area (ha)	Percent (%)	Area (ha)	Percent (%)
Ban tower	2192.203	4.67	44706.59	95.32
Charihan tower	6637.86	14.15	40260.92	85.84
Total visible area	8302.636	17.70	38596.15	82.29
Common visible area	999.3	2.13		

Results and discussions

We performed field survey by random forest sampling in the study area. The study area includes Conifers and Broad-leaved trees. Conifers like *Pinus roxburghii*, *Pinus wallichiana*, *Abies pindrow*, *Picea smithiana* have more tree volume due to their tall height as compared to broad leaved trees like *Olea spp*, *Quercus incana*, *Aesculus indica* (Mannan et al., 2018a). The results showed that the average density in the study area is 556.68 (± 128.19 std. dev.) trees per ha, while average BA is 40.27 (± 10.124 std. dev.) m²/ha, the average volume is 349.26 (± 111.06 std. dev.) m³/ha and mean DBH is 35.42 (± 15.54 std. dev.) cm.

Forest fires and CO₂ emission trend

We have obtained forest fire data for the last two decades that include fire origin location, size, date of occurrence, forest type and ignition cause from MFD. The historical record shows that accidental fires are 72.2% of the total fires, while 25% are deliberate and 2.6% are lightning-caused fires. Accidental fires mostly occur due to cigarette disposal in or around forests, careless fire handling during forest picnics, vehicle transportation, and the burning of farm residues along forests.

The increasing trend of forest fire has been observed in the study area, the average annual fire in the first decade (1998-2007) was 276 ha while it reached to 651 ha in the second decade (2008-2017), with the total 928.79 ha burned as shown in *Figure 5*.

The average dry organic matter in the forests was found to be 13837 (± 5774.64 std.dev.) g/m². The total estimated CO₂ emission in last 2 decades as obtained from the study is 145.60 (± 5369.68 std. dev.) Tg CO₂, with estimated average annual CO₂ being 7280 (± 5369 std. dev.) Gg CO₂. However, the largest fire events were observed in 2009 with 22799 Gg CO₂ emission. This was due to the fact that 2009 was recorded as driest summer year after 1980 (PMD, 2015). During the last two decades 788 (± 175 std. dev.) Gg CO₂ was emitted in the month of June followed by 25.40 (± 1.5 std. dev.) Gg CO₂ in May. The statistical analysis showed that average area burned in the first decade (1998-2007) was 27.69 ± 7.37^a (ha) which is significantly less than the second decade (2008-2017) which was 66.927 ± 7.37^b (ha), whereas the month of June found most critical for forest fire occurrence, with average forest fire of 23.13 ± 3.12^a (ha) significantly higher than 12.40 ± 3.12^b (ha) in May, while the occurrence of forest fire in the other months of the year was very less and showed non-significant relation with each other.

The historic fire record also showed that average net annual increase of CO₂ emission is 56%. According to Yi and Bao (2016) increasing temperatures and CO₂ concentration cause an increase in fuel availability. This increases the photosynthetic process which results into more plant growth and water use efficiency thus inducing more fires and CO₂ emission. *Figures 4* and *5* show that the rate of CO₂ emission increases steadily with increasing linear trend. Therefore, increases in temperatures exacerbate evapotranspiration which speeds-up the hydrological cycle (Finney et al., 2005). This ultimately causes more rainfall, vegetation growth, large fires and CO₂ emission. For instance, new settlements in Murree have been reported in the last decade, encroachment of forest area by land grabbers is a big issue, 1158 ha of forest land have encroached (Ashraf et al., 2014).

About 80% of fires occurred in areas accessible to humans, having road density and proximity to settlements, thus the patterns and occurrences of forest fires are related to human disturbances. Most of the fire events occurred in May and June burning over

653.2 ha, as shown in *Figure 5*. This may be attributed to the fact that, pine trees particularly *Pinus roxburghii* shed dry needles in the summer season and also because May and June constitute the hottest months. Additionally, this may be related to the fact that a ban on green felling was imposed in 1992. This put a halt to management activities such as thinning, pruning, line clearing and prescribed burning which in combination with burning are the most effective methods of fire prevention (Finney et al., 2005; Kuenzi et al., 2008)

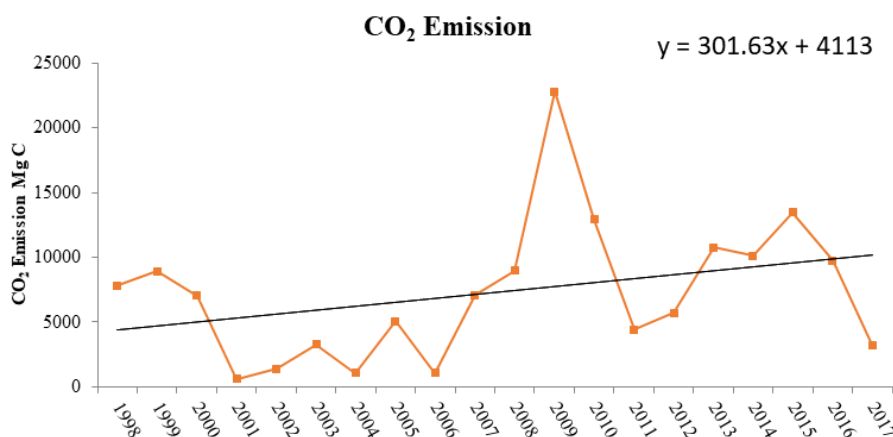


Figure 4. CO₂ emission trend

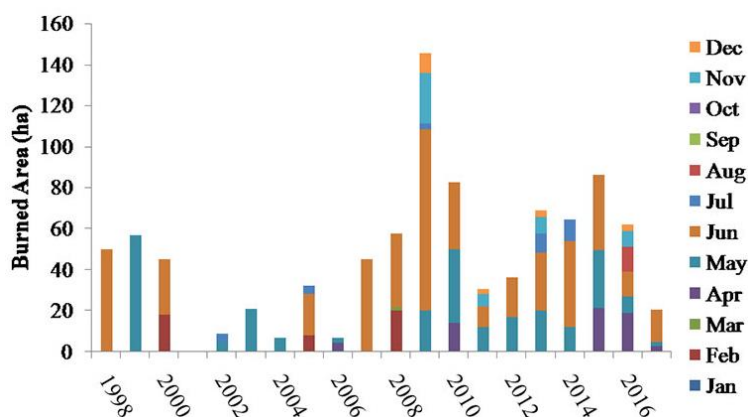


Figure 5. Forest fire trend

Fire risk zones and fire risk index

The Land-use map showed that 21.9% of the area includes DF which is in extreme risk zone, while 31.4% OF is in high-risk zone. Also, areas under low risks of fires AL are 6.6% and 39.9% which include water, roads, and barren lands (*Table 4* and *Fig. 6b*).

In the DF for instance, due to higher vegetation density, fuel is more available compared to the OF or BL. Thus, fire occurrence is more plausible and this is corroborated by another study by Martin et al. (2016) their study observed that forest fires are 70% more like to occur in dense vegetation as compared to sparse vegetation. The accuracy of land use map was assessed by formula as shown in *Equation 8*, and kappa statistics was 0.85.

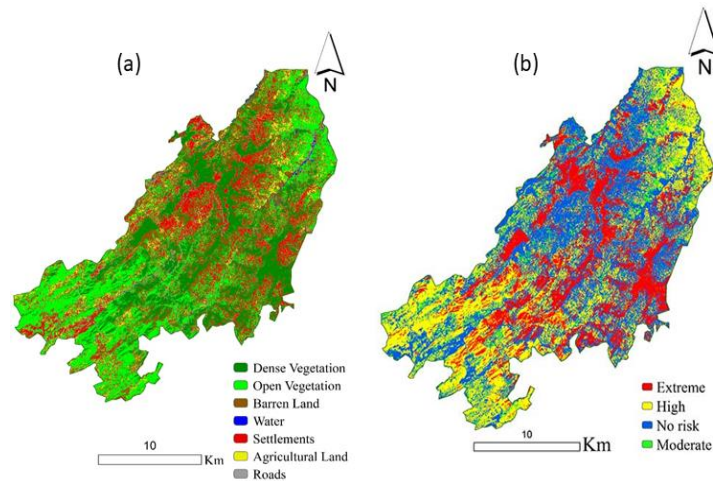


Figure 6. Land-use map (a) and land-use risk zones (b)

Similarly, from the forest distribution map, three forest types including broad-leaved evergreen forests, chirpine forests, and moist temperate forests were observed. Here, each forest type has its susceptibility level towards forest fires, and based on historical records obtained from the study area, Chirpine forests are most susceptible to forest fires mainly due to falling of dry needles in summer. Hence, their categorizations as extreme high-risk zones while the broad-leaved forests are categorized as high-risk zones and moist temperate forests as moderate risk zones. In a related study, Kumar et al., 2015 categorized Chirpine forests (*Pinus roxburghii*) as the major contributor to forest fires in Kangra region of Indian western Himalaya. Furthermore, the forest type map showed that more than half 51.14% of the area in the extreme risk zone, while 36.7% in a high-risk category and 12% in the moderate risk category (Fig. 7a).

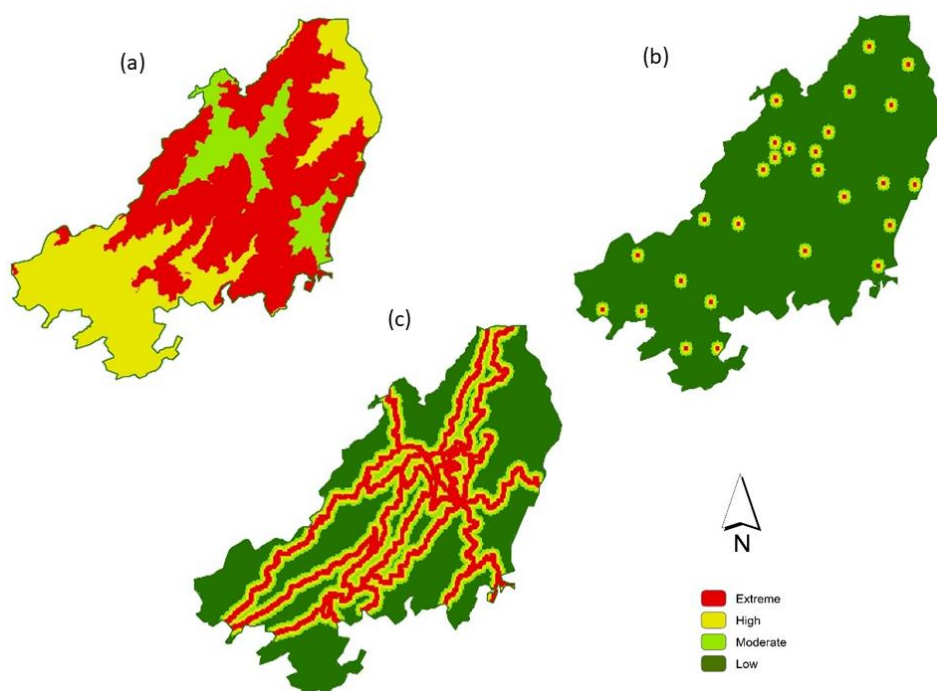


Figure 7. Risk zones of forest type (a), settlement center (b), roads (c)

However, in sub-tropical broad-leaved evergreen forest which is present at lower altitudes of Himalayan Mountains, fire ignition chances are slightly lower due to the association of many plant species. According to Ye et al. (2017), various broadleaf species are fire resistant especially in the eastern parts of China. At higher elevations of Himalayan mountains, the chances of fire occurrence are lower, due to climatic conditions, studies also showed that 85% of fire occurred at the elevation lower than 1000 m, hardly any fire was recorded above 4000 m (Martin et al., 2016),

Topography which includes slope and elevation is also an important role in the ignition and expansion of forest fires. Topography is an important factor in forest fire ignition and it was given much importance in studying forest fire causes in western United States (Liu et al., 2015). In slope aspect the southern (S) and south-west (SW) slopes are dry in nature due to the sun's direct impact thus leading to higher weights (Broszofske et al., 2007). Due to less moisture, high temperatures, robust winds and low fuel moisture, chances of fire ignitions are higher in southern aspects (Finney et al., 2005). Similarly, there are less chances of fire occurrence on north (N), north east (NE), west (W), and North West (NW) slope as sunrays not fall directly upon them. From the aspect risk map, 22.04% of the area faces the south and is thus located in extreme fire risk zones (S) and south-west (SW) slope. Meanwhile, 17.02% is located in the high-risk zone facing south-east (SE) slope and 50.66% is located in the moderate risk zone facing north-west, west, north east (NE) and east (E) as shown in *Figure 8c* and *Table 4*. Fire spreads quickly along steep slopes than gentle slopes because the flame angle is closer to the surface and where wind effects supply thermal energy through convection (Zhong et al., 2003). Similarly, steep slopes are more vulnerable for fire spreading slope map showed 0.26%, 12.51%, 59.43% and 27.78% in extreme, high, moderate and low risk zones respectively (*Fig. 8a* and *Table 4*).

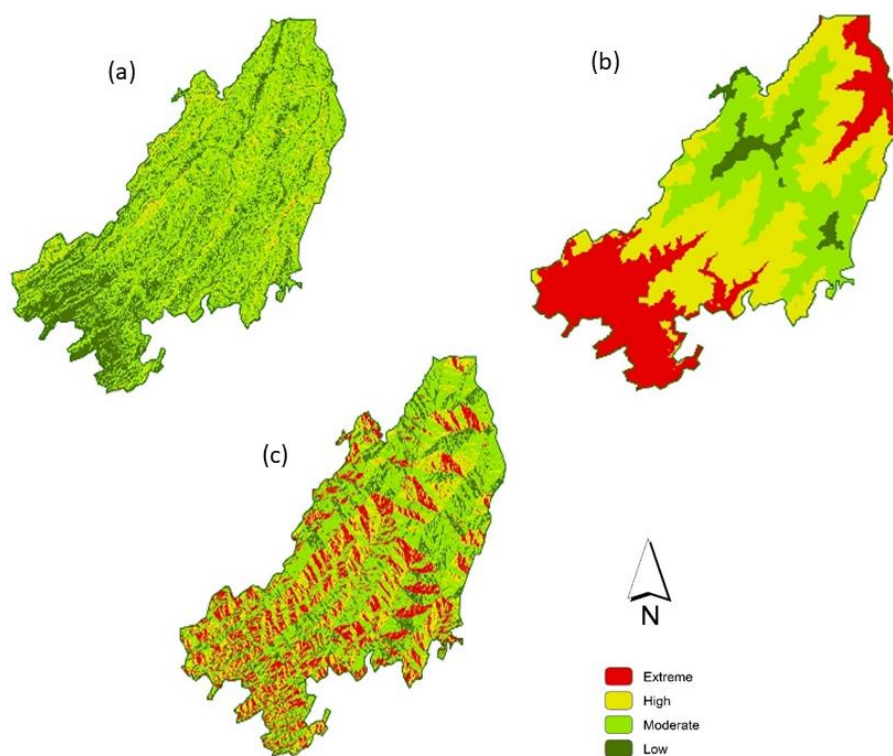


Figure 8. Risk zones of slope (a), elevation (b), aspect (c)

Table 4. Fire risk area in each variable zone

	Extreme		High		Moderate		Low		No risk	
	ha	%	ha	%	ha	%	ha	%	ha	%
Land-use	10285.73	21.9	14737.65	31.4	0	0	3123.31	6.6	18742.96	39.9
Forest type	23987.15	51.14	17246.80	36.7	5664.83	12	0	0	0	0
Aspect	10339.83	22.04	7982.24	17.02	23759.13	50.66	4817.587	10.27	0	0
Slope	122.96	0.26	5871.3	12.51	27875.08	59.43	13029.41	27.78	0	0
Elevation	13520.57	28.82	18621.54	39.7	12941.61	27.6	1814.96	3.86	0	0
Roads	9947.98	21.21	7471.46	15.93	5945.14	12.68	23520.23	50.16	0	0
Settlement	122.99	0.26	5871.3	12.51	13029.41	27.78	27875.08	59.43	0	0
FRZM	4376.93	9.33	21202.32	45.20	2443.60	5.21	18670.43	39.81	0	0

Human factors such as roads and settlements initiate forest with significant effects on forest ecosystem, land and water quality. The roads and settlement corridor map 0-100 m is rated as extreme risk zone, similarly 100-200 m, 300-400 m, and 400-500 m rated as high, moderate and low fire risk zones. However, 21.21% of the area of roads is located in the extreme risk zone, 15.93% in high risk and 12.68% in moderate risk zone (see Fig. 7c). Similarly, settlements map showed 0.26% to be located in the extreme risk zone, 12.51% in the high-risk zone and 27.78% in the moderate as shown in Figure 7b. Studies have also showed that the forest fires caused by human are often located in the proximity of roads and settlement corridors (Brosfoske et al., 2007; Maingi and Henry, 2007; Syphard et al., 2007). Road edges are also served as the habitat for some exotic plant species (Parendes and Jones, 2000). These species provide more combustible material fuel wood that are more easily ignited (Arienti et al., 2009). While it was also reported by Abdi et al. (2012) optimum roads network can decrease the chances of fire occurrence.

The visibility analysis showed that 4.67% of the study area is visible from the Ban fire tower, while 14.15% is visible from the Charihan fire tower. The combined visibility of the two towers is 17.70% and the total invisible area is 82.29%. The visibility of Charihan fire tower is 14.15% and Ban fire tower is 4.67% of the study area (see Table 3 and Fig. 9). The earlier detection of forest fire can minimize the forest damage up to 70%, however watch towers plays an important role for emergency response.

The Final Risk Zone Map (FRZM) (Fig. 10) was prepared by overlaying all the layers together according to the assigned weights in weighted overlay tool. FRZM showed 8.46% to be located in the extreme risk zone while the highest 46.30% area is in the high risk of the fire zone and the moderate risk zone has 5.22% and 40.02% in low risk zone, as shown in Table 5.

Table 5. Extent of fire risk zones

S No	Risk class	Area (ha)	Percent area (%)
1	Extreme	3998.513	8.46%
2	High	22059.487	46.30%
3	Moderate	2489	5.22%
4	Low	19053	40.02%

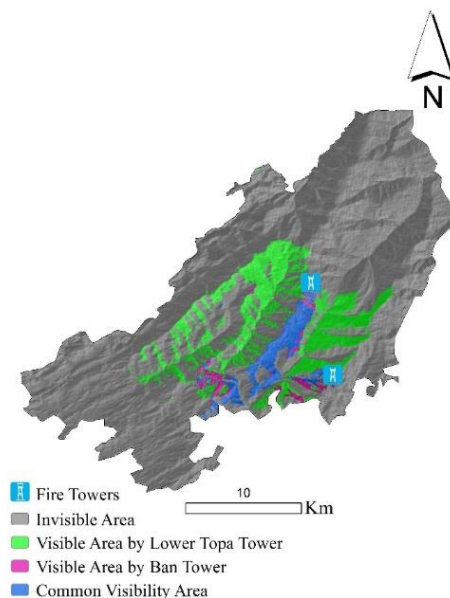


Figure 9. Visibility analysis map of fire watch towers

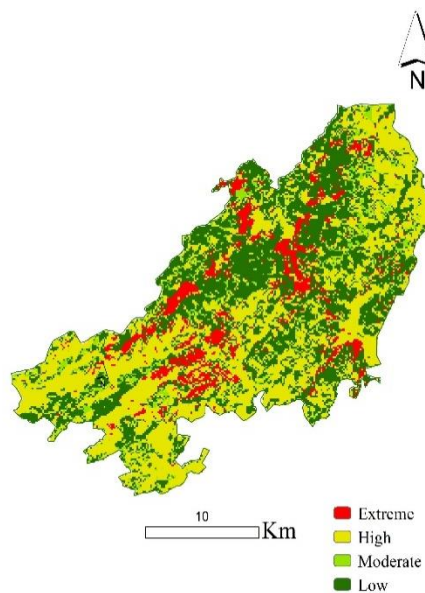


Figure 10. Land use fire risk zones

The FRZM shows fire vulnerability to be in more than half of the area is directly under the risk of fire. Finally, our FRZM was compared with actual fire-starting points, the majority of fire-starting points are in extreme and high fire risk zones.

Conclusion

The importance of forest fire risk zone assessment is well known but less attention has been paid towards the forest fire, CO₂ emission trend in subtropical and moist temperate forests of Pakistan.

In this study, we have calculated the CO₂ emission trend and forest fire risk zones. We found the CO₂ emission in the last three decades has been increased at accelerated rates. This increasing trend of CO₂ is directly linked with forest fire, and our study found that increase in forest fire due to more settlements, roads construction and human disturbance in the forest. Lightning caused forest fires are 2.6%, on other hand accidental fires 85% of the total fires. Although roads and settlements act as barriers to forest fires but 80% fires initiated from the corridors of roads and settlements.

This study integrates the historic fire record, ground sampling, remote sensing and GIS tools for fire risk zone assessment. The forest fire risk zone analysis showed that more than half of our study area is under extreme and high fire threat. This study provides risk assessment, factors and trends of forest fire, but further study on risk zone mapping of forest fire under predicted climate change is required, similarly forest fire trends and its effect on local climate is required, as well as the role of emergency response team and watch towers in fire management is required. This risk zone analysis will provide a broad picture to management authorities for combating this increasing fire trend and also suggest the future management.

Acknowledgements. This research was supported by the National Natural Science Foundation of China (No. U1710123), the Natural Science Foundation of Beijing (Key Program, No.6161001), and the medium and long-term project of the “Precision Forestry Key Technology and Equipment Research” (No. 2015ZCQ-LX-01).

REFERENCES

- [1] Abd El-Kawya, O. R., Rod, J. K., Ismail, H. A., Suliman, A. S. (2011): Land use and land cover change detection in the western Nile delta of Egypt using remote sensing data. – *Applied Geography* 31: 483-494.
- [2] Abdi, O., Shetaee, S. H., Shirvani, Z., Naghavi, M. R. (2012): The impact of forest management on forest fires in 2010 of Golestan Province by using GIS. – *Iran Journal for Range Protect Res* 2: 100-108.
- [3] Ahmad, A., Liu, Q. I. J., Nizami, S. M., Mannan, A., Saeed, S. (2018): Carbon emission from deforestation, forest degradation and wood harvest in the temperate region of hindukush himalaya, pakistan between 1994 and 2016. – *Land Use Policy* 78: 781-790. DOI: <https://doi.org/10.1016/j.landusepol.2018.07.009>.
- [4] Ali, Z. (2013): Missing the Forest for the Trees. – *DAWN*, 15 December.
- [5] Alonso, A., Fontenla, O., Guijarro, B., Hernández, E., Inmaculada, P., Andrade, M. A., Jiménez, E., Carballas, T. (2003): An intelligent system for forest fire risk prediction and fire fighting management in Galicia. – *Expert Systems with Applications* 25(4): 545-554. DOI: [https://doi.org/10.1016/S0957-4174\(03\)00095-2](https://doi.org/10.1016/S0957-4174(03)00095-2).
- [6] Amir, M., Liu, X., Ahmad, A., Saeed, S., Mannan, A., Atif, M., M. (2018): Patterns of biomass and carbon allocation across chronosequence of chir pine (*Pinus roxburghii*) forest in Pakistan: inventory-based estimate. – *Advances in Meteorology* Article ID 3095891. <https://doi.org/10.1155/2018/3095891>.
- [7] Andreae, M. O., Merlet, P. (2001): Emission of trace gases and aerosols from biomass burning. – *Global Biogeochemical Cycles* 15(4): 955-966. DOI: 10.1029/2000GB001382.
- [8] Arienti, M. C., Cumming, S. G., Krawchuk, M. A., Boutin, S. (2009): Road network density correlated with increased lightning fire incidence in the Canadian western boreal forest. – *International Journal of Wildland Fire* 18: 970-982.
- [9] Ashraf, I., Saeed, U., Shahzad, N., Gill, J., Parvez, S., Raja, A. (2014): Delineating Legal Forest Boundaries to Combat Illegal Forest Encroachments: A Case Study in Murree

- Forest Division, Pakistan. – In: Elmes, G. A., Roedl, G., Conley, J. (eds.) *Forensic GIS: The Role of Geospatial Technologies for Investigating Crime and Providing Evidence*. Springer Netherlands, Dordrecht, pp. 263-286.
- [10] Bacani, V. M. (2016): Geoprocessing Applied to Risk Assessment of Forest Fires in the Municipality of Bodoquena, Mato Grosso Do Sul. – *Revista Árvore* 40: 1003-1011.
- [11] Beckline, M., Yujun, S. (2014): Evaluating the effects of global environmental changes on ecosystems via Mycorrhizae, soil biota and plant traits. – *Applied Ecology and Environmental Sciences* 2(6): 135-140. DOI: 10.12691/aees-2-6-2.
- [12] Brosofske, K. D., Cleland, D. T., Saunders, S. (2007): Factors influencing modern wildfire occurrence in the Mark Twain National Forest, Missouri. – *Southern Journal of Applied Forestry* 31: 73-84.
- [13] Brown, S., Leugo, A. (1982): The storage and production of organic matter in tropical forests and their role in the global carbon cycle. – *Biotropica* 14: 161-187.
- [14] Chanthalath, X., Yong, L., Mukete, B., and Inthilath, S. (2017): Assessing the socioecological perspectives of eucalyptus cultivation and plantation expansion in Laos. – *Open Access Library Journal* 4: 424-430. DOI: <https://doi.org/10.4236/oalib.1104243>.
- [15] Dong, X., Li-min, D., Guo-fan, S., Lei, T., Hui, W. (2005): Forest fire risk zone mapping from satellite images and GIS for Baihe Forestry Bureau, Jilin, China. – *Journal of forestry research* 16(3): 169-174. DOI: 10.1007/BF02856809.
- [16] FAO (2015): *Global Forest Resources Assessment*. – Food and Agriculture Organization of the United Nations, Rome. <http://www.fao.org/3/a-i4808e.pdf>.
- [17] Finney, M. A., McHugh, C. W., Grenfell, I. C. (2005): Stand and landscape-level effects of prescribed burning on two Arizona wildfires. – *Canadian Journal of Forest Research* 35(7): 1714-1722. DOI: 10.1139/x05-090.
- [18] Giglio, L., Wan, Der, W., Randerson, J. T., Collatz, G. J., Kasibhatla, P. (2006): Global estimation of burned area using MODIS active fire observations. – *Atmos. Chem. Phys* 6(4): 957-974.
- [19] Hansen, M. C., Potapov, P. V., Moore, R., Hancher, M., Turubanova, S. A., Tyukavina, A., Townshend, J. R. (2013): High-resolution global maps of 21st-century forest cover change. – *Science* 342(6160): 850-853. DOI: 10.1126/science.1244693.
- [20] Harden, J. W., Trumbore, S. E., Stocks, B. J., Hirsch, A., Gower, S. T., O'Neill, K. P., Kasischke, E. S. (2000): The role of fire in the boreal carbon budget. – *Global Change Biology* 6(51): 174-184. DOI: 10.1046/j.1365-2486.2000.06019.x.
- [21] Haripriya, G. S. (2002): Biomass carbon of truncated diameter classes in Indian forests. – *Forest Ecology and Management* 168(1): 1-13. DOI: [https://doi.org/10.1016/S0378-1127\(01\)00729-0](https://doi.org/10.1016/S0378-1127(01)00729-0).
- [22] Harris, P. M., Ventura, S. J. (1995): The integration of geographic data with remotely sensed imagery to improve classification in an urban area. – *Photogrammic Engineering and Remote Sensing* 61: 993-998.
- [23] IPCC (2006a): *Inter-Governmental Panel on Climate Change (IPCC) Guidelines for National Greenhouse Gas Inventories*. – IPCC, Geneva.
- [24] IPCC (2006b): *IPCC Guidelines for National Greenhouse Gas Inventories, Prepared by the National Greenhouse Gas Inventories Programme (4)*. – IGES, Japan.
- [25] Ito, A., Penner, J. E. (2004): Global estimates of biomass burning emissions based on satellite imagery for the year 2000. – *Journal of Geophysical Research* 109(D14SO5) DOI: 10.1029/2003JD004423.
- [26] Iwan, S., Mahmood, A. R., Mansor, S., Mohamed, S., Nuruddin. (2004): GIS-grid-based and multi-criteria analysis for identifying and mapping peat swamp forest fire hazard in Pahang, Malaysia. – *Disaster Prevention and Management* 13(5): 379-386. DOI: 10.1108/09653560410568507.
- [27] Jaiswal, R. K., Mukherjee, S., Raju, K. D., Saxena, R. (2002): Forest fire risk zone mapping from satellite imagery and GIS. – *International Journal of Applied Earth*

- Observation and Geoinformation 4(1): 1-10. DOI: [https://doi.org/10.1016/S0303-2434\(02\)00006-5](https://doi.org/10.1016/S0303-2434(02)00006-5).
- [28] Krawchuk, M. A., Moritz, M. A., Parisien, M. A., Dorn, J., Hayhoe, K. (2009): Global pyrogeography: the current and future distribution of wildfire. – Plos One 4(4): 5102. DOI: [10.1371/journal.pone.0005102](https://doi.org/10.1371/journal.pone.0005102).
- [29] Kuenzi, A. M., Peter, Z., Sieg, Carolyn, H. (2008): Effects of fire severity and pre-fire stand treatment on plant community recovery after a large wildfire. – Forest Ecology and Management 255(3): 855-865.
- [30] Kumar, S., Meenakshi, D. B. G., Vandana, Kumar, A. (2015): Identifying triggers for forest fire and assessing fire susceptibility of forests in Indian western Himalaya using geospatial techniques. – Natural Hazards 78(1): 203-217. DOI: [10.1007/s11069-015-1710-1](https://doi.org/10.1007/s11069-015-1710-1).
- [31] Leblon, B. (2005): Monitoring forest fire danger with remote sensing. – Natural Hazards 35(3): 343-359. DOI: [10.1007/s11069-004-1796-3](https://doi.org/10.1007/s11069-004-1796-3).
- [32] Liu, Z., Wimberly, M. C. (2015): Climatic and landscape influences on fire regimes from 1984 to 2010 in the Western United States. – PLoS One 10: 1-20.
- [33] Maingi, J. K., Henry, M. C. (2007): Factors influencing wildlife occurrence and distribution in eastern Kentucky, USA. – International Journal of Wildland Fire 16: 23-33.
- [34] Malhi, Y. B. T., Phillips, O. L., Almeida, S., Alvarez, E., Arroyo, L., Chave, J., Czimczik, C. I., Fiore, A. D., Higuchi, N., Killeen, T. J., Laurance, S. G., Laurance, W. F., Lewis, S. L., Montoya, L. M., Lloyd, J. (2004): The above-ground coarse wood productivity of 104 Neotropical forest plots. – Global Change Biology 10: 563-559.
- [35] Mannan, A., Feng, Z., Ahmad, A., Liu, J., Saeed, S., Mukete, B. (2018a): Carbon dynamics with land use change in Margallah Hills National Park, Islamabad (Pakistan) from 1990 to 2017. – Applied Ecology and Environmental Research 16(3): 3197-3214.
- [36] Mannan, A., Zhongke, F., Khan, U. T., Saeed, S., Amir, M., Khan, M. A and Badshah, M. T. (2018b): Variation in tree biomass and carbon stocks with respect to altitudinal gradient in the Himalayan forests of Northern Pakistan. – Journal of Pure and Applied Agriculture JPAA-A-18-02.
- [37] Martin, D., Tomida, M., Meacham, B. (2016): Environmental impact of fire. – Fire Science Reviews 5(1): 5. DOI: [10.1186/s40038-016-0014-1](https://doi.org/10.1186/s40038-016-0014-1).
- [38] Mitchener, L. J., Parker, A. J. (2005): Climate, lightning and wildfire in the national forests of the southeastern United States: 1989-1998. – Physical Geography 26(2): 147-162. DOI: [10.2747/0272-3646.26.2.147](https://doi.org/10.2747/0272-3646.26.2.147).
- [39] Mukete, B., Sun, Y., Etongo, D., Sajjad, S., Ngoe, M and Tamungang, R. (2018a): Cameroon must focus on SDGs in its economic development plans. – Environment Science and Policy for Sustainable Development 60(2): 25-32.
- [40] Mukete, B., sun, Y., Etongo, D., Ekoungoulou, R., Folega, F., Sajjad, S., Ngoe, M., Ndiaye, G. (2018b): Household Characteristics and Forest Resources Dependence in the Rumpi Hills of Cameroon. – Applied Ecology and Environmental Research 16(3):2755-79.
- [41] Newbery, D. M. (2009): Philip, M. S. Measuring trees and forests. 2nd Ed. 1994. xiv + 310 pp. ISBN 0-85198-883-0 (pbk). CAB International, Wallingford, Oxon. Price: £24.50/US \$46.50. – Journal of Tropical Ecology 11(2): 204-204. DOI: [10.1017/S0266467400008658](https://doi.org/10.1017/S0266467400008658).
- [42] Parendes, L., Jones, J. (2000): Role of Light Availability and Dispersal in Exotic Plant Invasion along Roads and Streams in the H. J. Andrews Experimental Forest, Oregon. – Conservation Biology 14(1): 64-75.
- [43] PMD (2015): Rainfall Statistics of Islamabad. – PMD, Islamabad.
- [44] Saeed, S., Ashraf, M. I., Ahmad, A., Rahman, Z. (2016): The Bela Forest ecosystem of District Jhelum, A potential carbon sink. – Pakistan Journal of Botany 48(1): 121-129.
- [45] Saeed, S., Sun, Y., Beckline, M., Chen, I., Lai, Z., Mannan, A., Ahmad, A., Shah, S., Amir, M., Ullah, T., Khan, A., Akbar, F. (2018): Altitudinal gradients and forest edge

- effect on soil organic carbon in chinese fir (*Cunninghamia Lanceolata*): a study from Southeastern China. – *Applied Ecology and Environmental Research* 17(1): 745-757.
- [46] Saeed, S., Sun, Y., Beckline, M., Chen, L., Zhang, B., Ahmad, A., Mannan, A., Khan, A., Iqbal, A. (2019): Forest edge effect on biomass carbon along altitudinal gradients in Chinese Fir (*Cunninghamia lanceolata*): A study from Southeastern China. – *Carbon Management* 1-12.
- [47] Saranya, K. L., Reddy, C. S., Rao, P. P. (2016): Estimating carbon emissions from forest fires over a decade in Similipal Biosphere Reserve, India. – *Remote Sensing Applications: Society and Environment* 4: 61-67. doi.org/10.1016/j.rsase.2016.06.001.
- [48] Saugier, B., Roy, J., Mooney, H. A. (2001): Estimations of Global Terrestrial Productivity: Converging toward a Single Number? – In: Roy, J. et al. (eds.) *Terrestrial Global Productivity*. Academic Press, San Diego, pp. 543-55.
- [49] Seiler, W., Crutzen, P. J. (1980): Estimates of gross and net fluxes of carbon between the biosphere and the atmosphere from biomass burning. – *Climatic Change* 2(3): 207-247. DOI: 10.1007/BF00137988.
- [50] Shahzad, N., Saeed, U., Gilani, H., Ahmad, S. R., Ashraf, I., Irteza, S. M. (2015): Evaluation of state and community/private forests in Punjab, Pakistan using geospatial data and related techniques. – *Forest Ecosystems* 2(1): 7-15. DOI: 10.1186/s40663-015-0032-9.
- [51] Sheikh, M. I. (1993): *Trees of Pakistan*. – Peshawar Pakistan Forest Institute, Islamabad.
- [52] Simpson, I. J., Rowland, F. S., Meinardi, S., Blake, D. R. (2006): Influence of biomass burning during recent fluctuations in the slow growth of global tropospheric methane. – *Geophysical Research Letters* 33(22): 1011-1018. DOI: 10.1029/2006GL027330.
- [53] Syphard, A. D., Radeloff, V. C., Keeley, J. E., Hawbaker, T. J., Clayton, M. K., Stewart, S. I., Rogger, B. (2007): Human influence on California fire regimes. – *Ecological Applications* 17(5): 1388-1402.
- [54] Tanvir, A., Shahbaz, B., Suleri, A. (2006): Analysis of myths and realities of deforestation in northwest Pakistan: implications for forestry extension. – *International Journal of Agriculture and Biology* 8(1).
- [55] Tenzin, J., Wangchuk, T., Hasenauer, H. (2017): Form factor functions for nine commercial tree species in Bhutan. – *An International Journal of Forest Research* 90(3): 359-366. DOI: 10.1093/forestry/cpw044.
- [56] Thompson, M. P., Rodríguez, Y., Silva, F., Calkin, D. E., Hand, M. S. (2017): A review of challenges to determining and demonstrating efficiency of large fire management. – *International Journal of Wildland Fire* 26(7): 562-573. DOI: https://doi.org/10.1071/WF16137.
- [57] Vilen, T., Fernandes, P. M. (2011): Forest fires in Mediterranean countries: CO₂ emissions and mitigation possibilities through prescribed burning. – *Environment Management* 48(3): 558-567. DOI: 10.1007/s00267-011-9681-9.
- [58] Weber, R. M., Dunno, G. A. (2001): Riparian vegetation mapping and image processing techniques, Hopi Indian Reservation, Arizona. *Photogramm.* – *Engineering and Remote Sensing* 67(2): 179-186. DOI: citeulike-article-id: 2373717.
- [59] Weisse, M., Liz, G. (2017): Global Tree Cover Loss Rose 51% in 2016. – *Global Forest Watch*, 18 October.
- [60] Wekesa, C., Leley, N., Maranga, E., Kirui, B., Muturi, G., Mbuvi, M., Chikamai, B. (2016): Effects of forest disturbance on vegetation structure and above-ground carbon in three isolated forest patches of Taita hills. – *Open Journal of Forestry* 142-161. DOI: 10.4236/ojf.2016.62013.
- [61] Ye, T., Wang, Y., Guo, Z., Li, Y. (2017): Factor contribution to fire occurrence, size, and burn probability in a subtropical coniferous forest in East China. – *Plos One* 12(2): 0172110. DOI: 10.1371/journal.pone.0172110.
- [62] Yi, K., Bao, Y. (2016). Estimates of wildfire emissions in boreal forests of China. – *Forests* 7(8): 158.

- [63] Zhang, J. H., Yao, F. M., Liu, C., Yang, L. M., Boken, V. K. (2011): Detection, emission estimation and risk prediction of forest fires in china using satellite sensors and simulation models in the past three decades an overview. – *International Journal of Environmental Research and Public Health* 8(8): 3156-3178. DOI: 10.3390/ijerph8083156.
- [64] Zhong, M., Fan, W., Liu, T., Li, P. (2003): Statistical analysis on current status of China forest fire safety. – *Fire Safety Journal* 38(3): 257-269.